A Comparative Study of Morphological and Other Texture Features for the Characterization of Atherosclerotic Carotid Plaques

C.I. Christodoulou[1], E. Kyriacou[2], M.S. Pattichis[3],
C.S. Pattichis[2], and A. Nicolaides

[1] Cyprus Institute of Neurology and Genetics, P.O.Box 3462, 1683 Nicosia, Cyprus
cschr2@ucy.ac.cy
[2] Dept. of Computer Science, University of Cyprus, P.O.Box 20578, 1678 Nicosia, Cyprus
{ekyriac,pattichi}@ucy.ac.cy
[3] Dep. of Electrical and Computer Engineering, University of New Mexico, NM, USA
pattichis@eece.unm.edu

Abstract. The extraction of features characterizing the structure of atherosclerotic carotid plaques, obtained by high-resolution ultrasound imaging is important for the correct plaque classification and the estimation of the risk of stroke. In this study morphological features were extracted and compared with the well-known texture features spatial gray level dependence matrices (SGLDM), gray level difference statistics (GLDS) and the first order statistics (FOS) for the classification of 330 carotid plaques. For the classification the neural self-organizing map (SOM) classifier and the statistical k-nearest neighbor (KNN) classifier were used. The results showed that morphological and other texture features are comparable, with the morphological and the GLDS feature sets to perform slightly better than the SGLDM and the FOS features. The highest diagnostic yield was achieved with the GLDS feature set and it was about 70%.

1 Introduction

There are indications that the morphology of atherosclerotic carotid plaques, obtained by high-resolution ultrasound imaging, has prognostic implications [1-5]. Smooth surface, echogenicity and a homogenous texture are characteristics of stable plaques, whereas irregular surface, echolucency and a heterogeneous texture are characteristics of potentially unstable plaques. The extraction of features characterizing efficiently the structure of ultrasound carotid plaques is important for the correct plaque classification. The objective of this work was to investigate the usefulness of morphological features for the characterization of carotid plaques for the identification of individuals with asymptomatic carotid stenosis at risk of stroke. The developed system should be able, based on extracted morphological and other texture features to classify plaques into one of the following types: 1) symptomatic because of ipsilateral hemispheric symptoms, and 2) asymptomatic because they were not connected with ipsilateral hemispheric events. The aim is to identify subjects at risk of stroke.

2   Material

A total of 330 carotid plaque ultrasound images (194 asymptomatic and 136 symptomatic) were analyzed. The carotid plaques were labeled as symptomatic after one of the following symptoms was identified: 1) Stroke, 2) Transient Ischemic Attack (TIA) or 3) Amaurosis Fugax (AF). Two sets of data were selected: 1) for training the system, and 2) for evaluating its performance. For training the system 90 asymptomatic and 90 symptomatic plaques were used, whereas for evaluation of the system the remaining 104 asymptomatic and 46 symptomatic plaques were used. The ultrasound images were collected at the Irvine Laboratory for Cardiovascular Investigation and Research, Saint Mary's Hospital, UK, by two ultrasonographers using an ATL duplex scanner with a 7-4 MHz multifrequency probe. Longitudinal scans were performed using duplex scanning and color flow imaging [6].

Before processing, the images were standardized manually by linearly adjusting the image so that the median gray level value of the blood was 0, and the median gray level value of the adventitia (artery wall) was 190. The scale of the gray level of the images ranged from 0 to 255. This standardization using blood and adventitia as reference points was necessary in order to extract comparable measurements in case of processing images obtained by different operators or different equipment [6]. Following the image standardization, the expert physician using as guide their corresponding color blood flow images segmented the plaques manually. Figure 1 shows ultrasound images with the plaque region outlined.
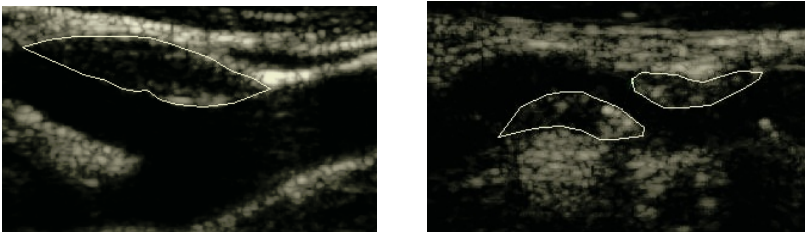

Fig. 1. Ultrasound images of the carotid artery with the atherosclerotic carotid plaques outlined

3   Feature Extraction and Selection

In order for the pattern recognition process to be tractable it is necessary to convert patterns into features, which are condensed representations of the patterns, containing only salient information. Features contain the characteristics of a pattern in a comparable form making the pattern classification possible. The extraction from the signal patterns of good features and the selection from them of the ones with the most discriminatory power can be very crucial for the success of the classification process. In this work morphological and other texture features were extracted from the segmented plaque images in order to be used for the classification of the carotid plaques.

3.1   Morphological Features

Morphological image processing allows us to detect the presence of specified patterns at different scales. We consider the detection of isotropic features that show no preference to particular directions. The simplest structural element for near-isotropic detection is the cross '+' consisting of 5 image pixels.

Thus, we considered pattern spectra based on a flat '+' structural element B. Formally, the Pattern Spectrum is defined in terms of the Discrete Size Transform (DST). We define the DST using [7, 8, 9]:

$$f \rightarrow (..., d_{-k}(f;B),...d_{-1}(f;B), d_0(f;B),...., d_1(f;B),......, d_k(f;B),....) \tag{1}$$

where

$$d_k(f;B) = \begin{cases} fokB - fo(k+1)B, k \geq 0 \\ f \bullet |k|B - f \bullet (|k|-1)B, k \leq 0 \end{cases} \tag{2}$$

o denotes an open operation, and $\bullet$ denotes the close operation. The grayscale DST is a multi-resolution image decomposition scheme, which decomposes an image f into residual images $f \circ kB - f \circ (k+1)B$, for $k > 0$, and $f \bullet |k|B - f \bullet (|k|+1)B$ for $k < 0$. The pattern spectrum of a grayscale image f, in terms of a structuring element B, is given by:

$$P_{f;B}(k) = \|d_k(f;B)\| = \begin{cases} \|fokB - fo(k+1)B\|, k \geq 0 \\ \|f \bullet |k|B - f \bullet (|k|-1)B\|, k \leq 0 \end{cases} \tag{3}$$

where

$$\|f\| = \sum_{x,y} f(x,y), \quad f(x,y) \geq 0 . \tag{4}$$

We note that in the limit, as $k \rightarrow \infty$, we have that the resulting image $f \circ kB - f \circ (k+1)B$ converges to the zero image. Also, we note that with increasing values of k, $f \circ kB$ is a subset of the original image. For $k \geq 0$, we may thus normalize the Pattern Spectrum by dividing by the norm of the original image $\|f\|$. Similarly, as $k \rightarrow \infty$, $\|f \bullet kB\|$ converges to $NM \max f(x,y)$, where it is assumed that the image is of size N by M. Hence, for $k < 0$, we can normalize the pattern spectrum by dividing by $NM \max f(x,y) - \|f\|$. Thus, to eliminate undesired variations, all the pattern spectra were normalized.

3.2   Texture Features

Texture refers to the spatial interrelationships and arrangement of the basic elements of an image. Visually, these spatial interrelationships and arrangements of the image

pixels are seen as variations in the intensity patterns or gray tones. Therefore texture features have to be derived from the gray tones of the image.

The following feature sets were computed:

(a) First Order Statistics (FOS):

1) Mean value, 2) Variance, 3) Median value, 4) Skewness, 5) Kurtosis, 6) Energy, 7) Entropy.

(b) Spatial Gray Level Dependence Matrices (SGLDM). The spatial gray level dependence (co-occurrence) matrices as proposed by Haralick et al. [10] are based on the estimation of the second-order joint conditional probability density functions that two pixels (k,l) and (m,n) with distance d in direction specified by the angle θ, have intensities of gray level i and gray level j. Based on the probability density functions the following texture measures [7] were computed:

1) Angular second moment, 2) Contrast, 3) Correlation, 4) Sum of squares: variance, 5) Inverse difference moment, 6) Sum average, 7) Sum variance, 8) Sum entropy, 9) Entropy, 10) Difference variance, 11) Difference entropy, and 12), 13) Information measures of correlation.

For a chosen distance d (in this work $d=10$ was used) and for angles $\theta = 0°$, $45°$, $90°$ and $135°$ we computed four values for each of the above 13 texture measures. In this work, the mean of these four values were computed for each feature and it was used for classification.

(c) Gray Level Difference Statistics (GLDS). The GLDS algorithm [11] uses first order statistics of local property values based on absolute differences between pairs of gray levels or of average gray levels in order to extract the following texture measures:

1) Homogeneity, 2) Contrast, 3) Energy, 4) Entropy, and 5) Mean.

The above features were calculated for displacements $\delta = (0, 1)$, $(1, 1)$, $(1,0)$, $(1,-1)$, where $\delta \equiv (\Delta x, \Delta y)$, and their mean values were taken.

3.3   Feature Selection

A simple way for calculating the discriminatory power of each individual feature can be defined by computing the distance between the two classes for each feature as:

$$dis = \frac{|m_1 - m_2|}{\sqrt{\sigma_1^2 + \sigma_2^2}} \tag{5}$$

where m_1 and m_2 are the mean values and σ_1 and σ_2 are the standard deviations of the two classes for each feature. The features with the highest discriminatory power are considered to be the ones with the greatest distance.

4   Plaque Classification

For the classification of the carotid plaques into symptomatic or asymptomatic two different classifiers were used: (i) the neural network self-organizing map (SOM) classifier [12] and (ii) the statistical K-Nearest Neighbor (KNN) classifier. All fea-

tures were normalized before use by subtracting their mean value and dividing with their standard deviation:

$$n(x_i)=(x_i-m_i) \, / \, \sigma_i \qquad (6)$$

where m_i is the mean value and σ_i is the standard deviation of the feature i .

4.1   The SOM Classifier

The SOM was chosen because it is an unsupervised learning algorithm where the input patterns are freely distributed over the output node matrix [12]. The weights are adapted without supervision in such a way, so that the density distribution of the input data is preserved and represented on the output nodes. This mapping of similar input patterns to output nodes, which are close to each other, represents a discretisation of the input space, allowing a visualization of the distribution of the input data. The output nodes are usually ordered in a two dimensional grid and at the end of the training phase, the output nodes are labeled with the class of the majority of the input patterns of the training set, assigned to each node.

In the evaluation phase, a new input pattern was assigned to the winning output node with the weight vector closest to the new input vector. In order to classify the new input pattern, the majority of the labels of the output nodes in a *RxR* neighborhood window centered at the winning node, were considered. The number of the input patterns in the neighborhood window for the two classes $m=\{1, 2\}$, (1=symptomatic, 2=asymptomatic), was computed as:

$$SN_m = \sum_{i=1}^{L} W_i N_{mi} \qquad (7)$$

where L is the number of the output nodes in the *RxR* neighborhood window with $L=R^2$ (e.g. $L=9$ using a 3x3 window), and N_{mi} is the number of the training patterns of the class m assigned to the output node i. $W_i=1/(2 \, d_i)$, is a weighting factor based on the distance d_i of the output node i to the winning output node. W_i gives the output nodes near to the winning output node a greater weight than the ones farther away (e.g. in a 3x3 window, for the winning node $W_i=1$, for the four nodes perpendicular to the winning node $W_i=0.5$ and for the four nodes diagonally located $W_i=0.3536$, etc). The evaluation input pattern was classified to the class m of the SN_m with the greatest value, as symptomatic or asymptomatic. In this work five different window sizes were tested: 1x1, 3x3, 5x5, 7x7, 9x9.

Figure 2 illustrates the distribution of the 180 plaques of the training set on a 10x10 SOM using as input the 5 best morphological features. The figure illustrates the degree of overlap between the two classes.

4.2   The KNN Classifier

The statistical k-nearest neighbor (KNN) classifier was also used for the classification of the carotid plaques. In the KNN algorithm, in order to classify a new input pattern,
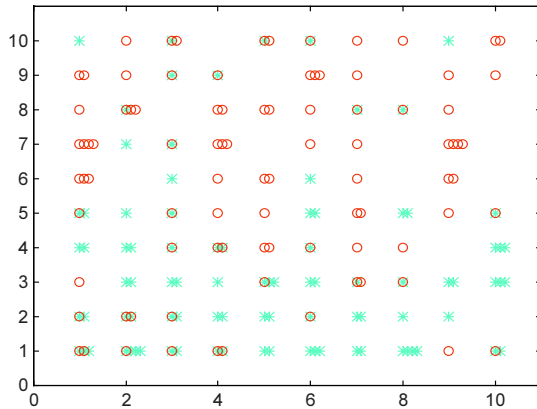
Fig. 2. Distribution of 180 carotid plaques of the training set (90 asymptomatic and 90 symptomatic) on a 10x10 SOM using as input the 5 best morphological features (* = asymptomatic, o = symptomatic). Similar plaques are assigned to neighboring output matrix nodes. A new plaque will be assigned to one winning output node and will be classified based on the labels of the neighboring nodes in a *RxR* neighborhood window. The output nodes near to the winning node are given a greater weight than the ones farther away.

its *k* nearest neighbors from the training set are identified. The new pattern is classified to the most frequent class among its neighbors based on a similarity measure that is usually the Euclidean distance. In this work the KNN carotid plaque classification system was implemented for different values of $k = 1, 3, 5, 7, 9, 11, 19$ and it was tested using for input the different feature sets.

5   Results

A total of 330 ultrasound images of carotid atherosclerotic plaques were analyzed and four different feature sets (morphological, FOS, SGLDM and GLDS) were extracted from the manually segmented plaque images as described in section 3. The morphological algorithm extracted 98 features from the plaque images. Using the entire pattern spectra for classification yielded poor results. Using Eq. 5 the number of features used was reduced to only five, which proved to yield satisfactory classification results. The selected features represent the most significant normalized pattern spectra components. We determined that small features due to: $P_{1,'+'}$, $P_{2,'+'}$, $P_{3,'+'}$, $P_{-4,'+'}$ and $P_{-5,'+'}$ (see Eq. 3) yield the best results. It is noted the good performance of $P_{1,'+'}$, which may be susceptible to noise but it is also the feature that is most sensitive to turbulent flow effects around the carotid plaques. Table 1 tabulates the statistics for the five selected morphological features, for the two classes and their interclass distance as computed with Eq. 5.

Table 1. Statistical analysis of the five best morphological features computed from the 330 (194 asymptomatic and 136 symptomatic) ultrasound images of carotid plaques. For each feature the mean and standard deviation were computed for the asymptomatic group and for the symptomatic group. The distance between the symptomatic and the asymptomatic groups was computed as described in Eq. 5

| *Feature* | *Asymptomatic* | | *Symptomatic* | | *Distance* |
	Mean M_1	*Std* σ_1	*Mean* M_2	*Std* σ_2	$dis = \dfrac{\lvert m_1 - m_2 \rvert}{\sqrt{\sigma_1^2 + \sigma_2^2}}$
$P_{1,'+'}$	0.0249	0.0229	0.0433	0.0407	0.3934
$P_{3,'+'}$	0.1355	0.0870	0.1922	0.1218	0.3787
$P_{2,'+'}$	0.0713	0.0520	0.1102	0.0888	0.3782
$P_{-4,'+'}$	0.0119	0.0084	0.0080	0.0061	0.3701
$P_{-5,'+'}$	0.0158	0.0109	0.0108	0.0079	0.3675

For the classification task, the neural SOM classifier and the statistical KNN classifier were implemented. For training the classifier, 90 symptomatic and 90 asymptomatic plaques were used, whereas for evaluation of the system the remaining 104 asymptomatic and 46 symptomatic plaques were used. Table 2 tabulates the diagnostic yield for the SOM classifier for the different feature sets and for different neighborhood window sizes on the self-organizing map. Table 3 tabulates the diagnostic yield of the KNN classifier for the different feature sets, for different values of k. The diagnostic yield is defined as the percentage of the correctly classified plaques to the total number of the tested plaques. The estimated success rate for the two classes was about similar.

The unsupervised neural SOM classifier was implemented with a 10x10 output node architecture and it was trained for 5000 learning epochs. In order to obtain a more reliable estimate of the diagnostic yield, the SOM was trained and evaluated three times and the average of the three runs was used. Different neighborhood window sizes were tested, where larger window sizes tend to yield higher success rate. The significantly lower success rate for the 1x1 window size is attributed to the many 'undefined' cases where the evaluation input pattern was assigned to a node on the SOM (s. Fig. 2), where no training patterns were assigned during the training phase. The highest diagnostic yield was 69.6% and it was obtained with a 9x9 window size, using as input the GLDS feature set. On average, the results with the highest diagnostic yield were obtained by the GLDS feature set, which was 64.6%, followed by the morphological feature set with a diagnostic yield of 62.9%, the SGLDM with 62.2% and the FOS with 59.9%.

For comparison reasons the statistical KNN classifier was also implemented for different values of k, which also performed well. The best diagnostic yield was 68.7% and it was obtained with a $k=3$, using as input the morphological feature set. In average, the best results were obtained by the morphological feature set which was 66.3%, followed closely by the GLDS feature set with a diagnostic yield of 65.6%, the FOS with 63.9% and the SGLDM with 63.8%. Overall the classification results

Table 2. Diagnostic yield (%) of the SOM classifier for the different feature sets and different neighborhood window sizes on the self-organizing map

Window Size	Morphological	FOS	SGLDM	GLDS
1x1	52.4	40.5	44.2	50.0
3x3	66.7	61.6	66.0	66.0
5x5	64.7	65.8	64.4	68.0
7x7	64.7	66.2	67.8	69.3
9x9	65.8	65.5	68.7	69.6
Average	*62.9*	*59.9*	*62.2*	*64.6*

Table 3. Diagnostic yield (%) of the KNN classifier for the different feature sets, for different values of k

K	Morphological	FOS	SGLDM	GLDS
1	62.7	60.0	62.7	65.3
3	68.7	63.3	58.7	64.0
5	66.7	63.3	67.3	62.7
7	68.0	65.3	62.7	68.0
9	64.0	62.0	64.7	67.3
11	66.7	67.3	66.0	66.7
19	67.3	66.0	64.7	65.3
Average	*66.3*	*63.9*	*63.8*	*65.6*

for the two classifiers are comparable, with the morphological and the GLDS feature sets to perform slightly better than the SGLDM and the FOS features.

6   Discussion

In this study the usefulness of morphological features is investigated for the characterization of carotid plaques for the identification of individuals with asymptomatic carotid stenosis at risk of stroke. Previous work [4, 5] has shown that texture features can successfully be used for carotid plaque classification. In this work it is shown that morphological features are compare well with the most successful texture feature sets and provide an additional tool for the identification of individuals at risk of stroke. In future work the extracted morphological features will be extended to investigate the classification performance of larger components, and linear, directional structural elements. Also other feature selection methods such as principal component analysis and/or moments of pattern spectra can be considered in future studies, for the selection of the features with the highest discriminatory power. It is hoped that these enhancements will lead to a higher classification performance.

  In conclusion, the results in this work show that it is possible to identify a group of patients at risk of stroke based on morphological and other texture features extracted from high resolution ultrasound images of carotid plaques. This group of patients may benefit from a carotid endarterectomy whereas other patients may be spared from an unnecessary operation. Because of the difficulty of the problem and the high

degree of overlap of the symptomatic and asymptomatic classes, the above results should be verified with more images from more patients. Furthermore other source of information may be used for classification, for example information obtained by a 3-dimensional reconstruction of the carotid plaque, which may lead to a better diagnostic yield.

Acknowledgements

References

1. Elatrozy T., Nicolaides A., Tegos T., Griffin M., "The Objective Characterisation of Ultrasonic Carotid Plaque Features", *Eur J Vasc Endovasc Surg 16*, pp. 223-230, 1998.
2. Wilhjelm J.E., Gronholdt L.M., Wiebe B., Jespersen S.K., Hansen L.K., Sillesen H., "Quantitative Analysis of Ultrasound B-Mode Images of Carotid Atherosclerotic Plaque: Correlation with Visual Classification and Histological Examination", *IEEE Trans. on Medical Imaging,* Vol. 17, No. 6, pp.910-922, December 1998.
3. Polak J., Shemanski L., O'Leary D., Lefkowitz D., Price T., Savage P., Brand W., Reld C., "Hypoechoic Plaque at US of the Carotid Artery: An Independent Risk Factor for Incident Stroke in Adults Aged 65 Years or Older", *Radiology*, Vol. 208, No 3, pp. 649-654, Sept. 1998.
4. Christodoulou C.I., Pattichis C.S., Pantziaris M., Tegos T., Nicolaides A., Elatrozy T., Sabetai M., Dhanjil S., "Multi-feature texture analysis for the classification of carotid plaques", *Int. Joint Conf. on Neural Networks IJCNN '99*, Washington DC, July, 1999.
5. Christodoulou C.I., Pattichis C.S., Pantziaris M., Nicolaides A., "Texture Based Classification of Atherosclerotic Carotid Plaques", to be published in *IEEE Trans. on Medical Imaging,* 2003.
6. Elatrozy T., Nicolaides A., Tegos T., Zarka A., Griffin M., Sabetai M., "The effect of B-mode ultrasonic image standardisation on the echogenicity of symptomatic and asymptomatic carotid bifurcation plaques", *International Angiology*, Vol. 17, No 3, pp. 179-186, Sept. 1998.
7. Dougherty E.R., *An Introduction to Morphological Image Processing*, Belingham, Washington, SPIE Optical Engineering Press, 1992.
8. Dougherty E. R., Astola J., *An Introduction to Nonlinear Image Processing*, Belingham, Washington, SPIE Optical Engineering Press, 1994.
9. Maragos P., "Pattern spectrum and multiscale shape representation", *IEEE Trans. on Pattern Analysis and Machine Intelligence*, 11:701 715, 1989.
10. Haralick R.M., Shanmugam K., Dinstein I., "Texture Features for Image Classification", *IEEE Trans. on Systems, Man., and Cybernetics,* Vol. SMC-3, pp. 610-621, Nov. 1973.
11. Weszka J.S., Dyer C.R., Rosenfield A., "A Comparative Study of Texture Measures for Terrain Classification", *IEEE Trans. on Systems, Man. & Cybern.,* Vol. SMC-6, April 1976.
12. Kohonen T., "The Self-Organizing Map", *Proceedings of the IEEE*, Vol. 78, No. 9, pp. 1464-1480, Sept. 1990.